Torque Ripple Reduction in Direct Torque Control of Induction Motor Drives

Chuen Ling Toh, Nik Rumzi Nik Idris, *Senior Member, IEEE* and Abdul Halim Mohd Yatim, *Senior Member, IEEE*

***Abstract*--This paper gives an overview to the principle of Direct Torque Control (DTC) of Induction Machines (IM) drives. A summary to the various techniques of torque ripple reduction followed by a proposed simple method to reduce the torque ripple is also presented. Modeling and design methodology of this proposed method are given. Simulations of the proposed controllers were performed using MATLAB/SIMULINK simulation package. The results show that the controllers have managed to reduce the torque ripple significantly.**

***Keywords*--torque ripple, DTC, motor drives.**

I. Introduction

OVER the last couple of decades, field oriented control (FOC) of IM was introduced in the industry applications where precise and fast control of toque and/or speed is required. The basic arrangement of FOC composed of a co-ordinate transformer, a pulse width modulator (either voltage or current control) and a voltage source inverter (VSI). When compared to the scalar control method of IM (e.g. simpler constant V/Hz), FOC is far superior in terms of dynamic torque response, in the expense of far more complicated control system. The major problems usually associated with FOC technique is to estimate the flux position used in the algorithm. Various techniques were introduced with most of them tried to avoid the use of mechanical speed sensors (speed sensorless), which is known to reduce robustness and increase costs. Until now, speed sensorless operation of FOC induction motor drives still remains a challenging research area.

Another control technique for induction motor drives for an excellent performance, known as direct torque control (DTC) was introduced more than a decade ago. This control technique is capable of giving a fast and good dynamic torque response and can be considered as an alternative to the FOC [4][5]. The main features of DTC, which finds it more attractive than the FOC is that, it does not require frame transformations and mechanical speed sensor. Its control structure is simple as shown by the basic configuration of DTC in Fig 1, consisting of DTC controller, torque and flux calculator, and VSI. The DTC controller is made of selection table and hysterisis comparator, which are easy to implement. Nonetheless, DTC control technique in its basic configuration suffers from two major problems: 1) variable switching frequency and 2) high torque ripple. Several researchers have proposed variations to the basic DTC configurations as originally proposed in [1] with the aim of solving these two basic problems. Most of the methods introduced have indirectly reduced the torque ripple by increasing the switching frequency. The problem of variable switching frequency, on the other hand, was overcome by removing the hysteresis comparators, which are the root cause to the problem. The used of these various techniques however, have somehow increase the complexity of the control technique in DTC and hence diminish the main feature of DTC, which is simple control structure. This paper introduces two simple controllers for the torque and flux loops, which replaces the conventional hysteresis comparators. The controllers work based on waveform comparisons and hence retained the simple control structure of the DTC.

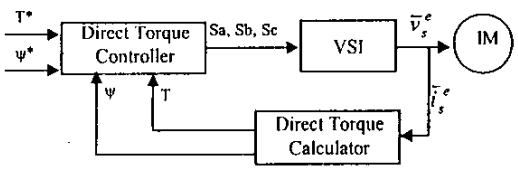

Fig. 1. Basic block of DTC

This paper is divided into 5 sections. Section 2 gives an overview on the principle operations. Section 3 briefly reviews the methods of torque ripple reduction. The new technique of torque ripple reduction is introduced in section 4. Some simulations results are discussed in section 5. Finally, conclusions are given in section 6.

II. Principles Of DTC

Theoretically, if a three phase VSI is connected to an IM, there can be eight possible configurations of six switching devices within the inverter. As a result, there are eight possible input voltage vectors to the IM. The eight voltage vectors, two of which are zero vectors, are depicted in Fig 2.

The authors are with the Department of Energy Conversion, Faculty of Electrical Engineering, Universiti Teknologi Malaysia, 81310 UTM Skudai, Johor Bahru, Malaysia.
(Email: tohchuenling@yahoo.com, nikrumzi@iecc.org, halim@iecc.org)

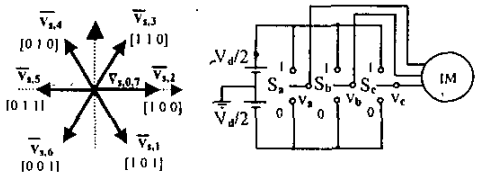

Fig. 2. Voltage vectors for 3-phase VSI

DTC utilizes the eight possible stator voltage vectors, two of which are zero vectors, to control the stator flux and torque to follow the reference values within the hysteresis bands. The voltage space vector of a three-phase system is given by:

$$\bar{v}_s(t) = \tfrac{2}{3}\left(v_{sA}(t) + a v_{sB}(t) + a^2 v_{sC}(t)\right), \quad \text{where } a = e^{j\frac{2}{3}\pi} \qquad (1)$$

Where v_{sA}, v_{sB}, and v_{sC} are the phase voltages. For the switching VSI, it can be shown that for a DC link voltage of V_d, the voltage space vector is given by:

$$\bar{v}_s(t) = \tfrac{2}{3} V_d\left(S_a(t) + S_b(t)a + S_c(t)a^2\right), \quad \text{where } a = e^{j\frac{2}{3}\pi} \qquad (2)$$

$S_a(t)$, $S_b(t)$ and $S_c(t)$ are the switching functions of each leg of the VSI, such that,

$$S_i = \begin{cases} 1 & \text{when upper switch is on} \\ 0 & \text{when lower switch is on} \end{cases} \qquad i = a,b,c$$

A. Direct Flux Control

The IM stator voltage equation is given by:

$$\bar{v}_s = R_s \bar{i}_s + \frac{d\bar{\psi}_s}{dt} \qquad (3)$$

Where $\bar{v}_s$, $\bar{i}_s$, and $\bar{\psi}_s$ are the stator voltage, current and stator flux space vectors respectively. According to equation (3), if the stator resistance is small and can be neglected, the change in stator flux, $\Delta\bar{\psi}_s$ will follow the stator voltage, i.e.,

$$\Delta\bar{\psi}_s = \bar{v}_s \Delta t \qquad (4)$$

This simply means that the tip of the stator flux will follow that of the stator voltage space vector multiplied by the change in time. Hence if the stator flux space vector (magnitude and angle) is known, it locus can be controlled by selecting appropriate stator voltage vectors. In DTC the stator flux space vector is obtain by calculation utilizing the motor terminal variables (stator voltages and currents). The stator flux is forced to follow the reference value within a hysteresis band by selecting the appropriate stator voltage vector using the hysteresis comparator and selection table.

B. Direct Torque Control

As shown by Takahashi [4], under a condition of a constant mechanical frequency and stator flux magnitude, when a step increase in the stator angular frequency is applied at t=0, the rate of change of torque at time t=0 is proportional to the slip frequency of the stator flux with respect to the rotor. Thus,

$$\left.\frac{dT}{dt}\right|_{t=0} \alpha \left.\omega_{sl}\right|_{t=0} \qquad (5)$$

Where ω_{sl} is the angular slip frequency of the stator flux with respect to the rotor mechanical frequency. This means that the rate of change of torque can be made positive or negative regardless of whether the stator flux is increasing or decreasing. By selecting the appropriate voltage vector, the torque can be made to swing within its upper and lower bands. If the stator flux space vector plane is divided into six sectors or segments (Figure 3) and each sector is further divided into two sub-sectors *a* and *b*, a set of table or rules of which voltage vector should be chosen in a particular sub-sector (either to increase stator flux or to reduce stator flux and either to increase torque or to reduce torque) can be constructed; such table is given by Table 1.

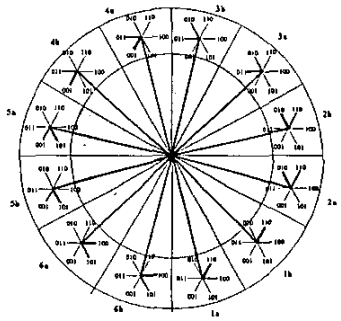

Fig. 3. Six sectors of stator flux plane.

TABLE I
VOLTAGE VECTORS FOR COUNTERCLOCKWISE ROTATION OF STATOR FLUX

		Sector I		Sector II		Sector III		Sector IV		Sector V		Sector VI	
		a	b	a	b	a	b	a	b	a	b	a	b
Inc Flux	*Inc T*	**100** 101	**100**	**110** 100	**110** 110	**010** 110	**010**	**011** 010	**011**	**001** 011	**001**	**101** 001	**101**
	Dec T	001 **000**	001 101 **000**	101 **111**	101 100 **111**	100 **000**	100 110 **111**	110 **111**	110 010 **111**	010 **000**	010 011 **111**	011 **111**	011 001 **111**
Dec Flux	*Inc T*	**110**	**110** 010	**010**	**010** 011	**011**	**011** 001	**001**	**001** 101	**101**	**101** 100	**100**	**100** 110
	Dec T	011 010 **000**	011 **111**	001 011 **111**	001 **000**	101 001 **000**	101 **000**	100 010 **000**	100 **000**	110 100 **000**	110 **111**	010 110 **111**	010 **000**

III. Overview Of Torque Ripple Reduction

A widely adopted method to reduce the torque ripple and at the same time maintaining a constant switching frequency is by removing the hysteresis comparators and by performing the switching at regular intervals. Instead of applying a single voltage vector for the whole sampling period, two or more voltage vectors are applied. Therefore the desired stator voltage can be synthesized by choosing the appropriate duty cycle or voltage vectors. In [6]-[9], the switching periods are sub–divided into two states and the difference between the various methods is only on the way of the duty cycles are calculated, such as using predictive control [6], using equation for minimum average torque ripple [7] and also fuzzy logic [8], [9]. Another approach is to use space vector modulation (SVM) technique to synthesize the desired stator voltage. In [5], [14], [15], a conventional SVM is used whereas in [10], the so-called discrete SVM is used whereby the switching period is equally divided into three equal durations. In conventional SVM, there will be two active and one zero voltage vectors applied within a switching period. With discrete SVM [10], the three voltage vectors applied within the switching period are selected using a modified look-up table and a five level hysteresis comparator.

By sub-dividing the switching period into two or more states, the switching frequency is effectively increased and therefore the torque ripple is also reduced. The various method of switching techniques in DTC is summarized in Fig. 4, which shows a typical torque and the corresponding three-phase inverter voltage waveforms, assuming the orientation of the stator flux is in sector 5. According to Table 1, the preferable voltage vectors to increase and to reduce the flux while at the same time to increase the torque in this sector, are [001] and [101] respectively. Reducing torque is achieved with zero voltage vectors (either [000] or [111]). Fig. 4(a) shows the torque waveforms for hysteresis-based controller with the width of the hysteresis marked as ΔT. Due to the delay in the microprocessor implementation or sensors, the torque overshoot and undershoot beyond and below the hysteresis bands will occur. According to (8), the positive slope is high at low speed, which will increase the possibility of the torque touching the upper band, thus selecting the reverse voltage to reduce the torque. In Fig. 4(b), fixed switching is employed but with the whole sampling period applied with a single voltage vector. Evidently, this technique will result in a high torque ripple with an additional torque oscillation [6]. Fig 4(c) shows the controlled duty cycle method in which various methods [6]-[9] can be used to calculate the duty cycle, δ, for every sampling period, T_s. The method, which synthesizes the voltage using SVM technique, is depicted in Fig. 4(d). The fixed switching frequency methods require fast processor for realization since the duty cycles or voltage vectors need to be calculated for every sampling period, particularly when small sampling period is required for appreciably small torque ripple. This is normally accomplished using fast digital signal processor. On the other hand, the hysteresis-based DTC drive as initially proposed in [1], has very simple structure and operates based on waveform comparisons. The simple structure of the controller is demonstrated in [1] whereby the realization of it is achieved using analog circuit. However, it suffers a major problem of variable switching frequency. The proposed controller, which will be introduced in the next section, is based on waveform comparisons. In spite of it simple structure and hence implementation, the proposed method managed to produce constant switching frequency and reduced torque ripple. The torque hysteresis comparator is completely removed and replaced with the proposed controller. The proposed controller will have the same task as the conventional 3-level hysteresis comparator, therefore the same look–up table to select the suitable voltage vectors as the one used with the conventional hysteresis-based controller, can be used.

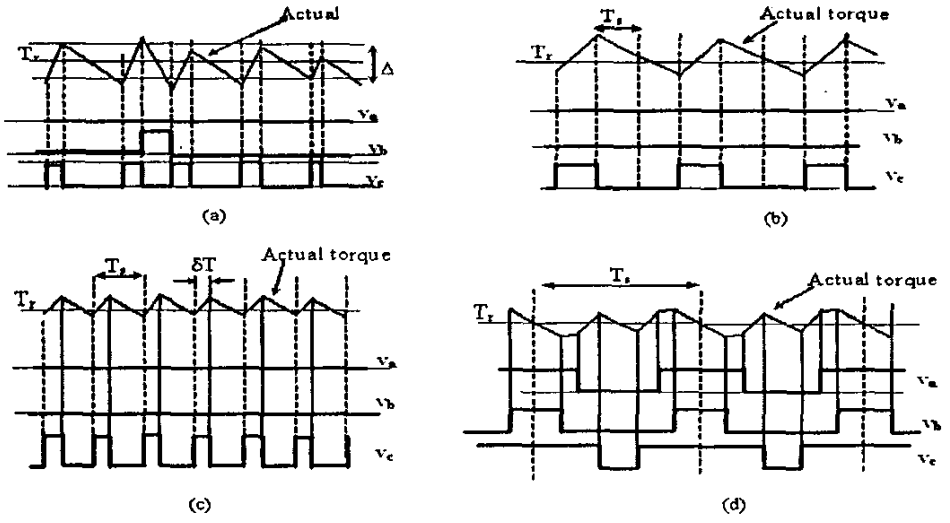

Fig. 4 Various switching strategies in DTC. (a) Hysteresis–based controller, (b) Fixed switching torque, (c) Fixed switching torque with controlled duty ratio, (d) fixed switching torque with space vector modulation

IV. Proposed Controllers

The core of these proposed controllers is based on the comparison between the compensated error signals with high frequency triangular waveform. It is believed that the torque ripple is minimized whereas a constant high switching frequency will also be achieved.

A. Proposed Torque Controller

The proposed torque controller consists of two triangular waveform generators, two comparators and a PI controller as shown in Fig. 5. The two triangular waveforms (which will be referred to as upper and lower carriers) are 180°. out of phase with each other. The absolute values of the DC offsets for upper and lower carriers are set to half of its peak-peak value; the upper dc offset is positive while the lower is negative. In principle, the output of the proposed torque controller is similar to that of the three level hysteresis comparator [1], which can be either of three states: –1, 0 or 1.

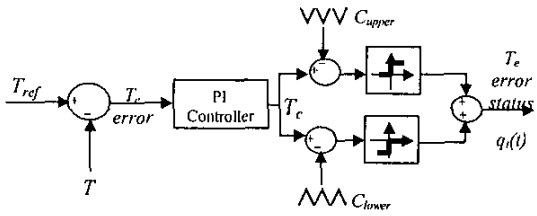

Fig. 5 Proposed torque controller

The value of the instantaneous output of the torque controller – named as *torque error status* and designated by $q(t)$ is given by :

$$q(t) = \begin{cases} 1 & for \quad T_{pi} \geq C_{upper} \\ 0 & for \quad C_{lower} < T_{pi} < C_{upper} \\ -1 & for \quad T_{pi} \leq C_{lower} \end{cases} \tag{6}$$

The average torque error status, $\bar{q}(t)$, is defined as *continuous duty ratio* and is denoted by d(t). The average is taken over an interval T_{tri}, which is the period of the trangular carrier waveform. It is defined by

$$d(t) = \frac{1}{T_{tri}} \int_{t}^{t+T_{tri}} q(t)\, dt \tag{7}$$

The values of the PI controller parameters are chosen based on the linear analysis of the controller in Fig. 5. Averaging and linearizing the torque equations obtain the linear model, which is given by [12]. It can be shown that [11] the positive and negative torque slope equations are given by (8) and (9) respectively:

$$\frac{dT_e^+}{dt} = -A_t T_e + B_t v_s^{\psi_s} + K_t\left(\frac{\omega_s}{d} - \omega_r\right) \tag{8}$$

$$\frac{dT_e^-}{dt} = -A_t T_e - K_t \omega_r \tag{9}$$

where $A_t = \frac{1}{\sigma\tau_{rr}}$, $B_t = \frac{3p}{4}\frac{L_m}{\sigma L_s L_r}\psi_s$ and $K_t = \frac{3p}{4}\frac{L_m}{\sigma L_s L_r}\psi_s\psi_r^{\psi_s}$

Averaging and linearizing equations (8) and (9), and with further simplifications, it can be shown that [11],

$$\frac{dT_e}{dt} = -AT_e + Bv_s^{\psi_s} d + K_1\left(\omega_{slip}\right) \tag{10}$$

Based on (10), the transfer function between d and T_e can be obtained by setting the slip frequency to zero. It can also be shown that the transfer function between the output of the PI controller, T_{pi} and the averaged duty ratio d is given by a reciprocal of the peak-peak triangular carrier, $C_{p\text{-}p}$. Thus the overall small signal block diagram of the proposed torque controller of Fig. 5 with averaged, linearized torque equation is shown in Fig. 6.

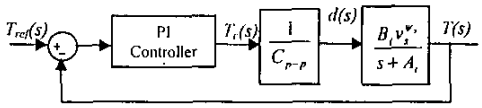

Fig. 6 Averaged and linearised torque loop

The values of the PI controller's parameters are chosen based on the following constraints:

- The absolute slope of equation (8) and (9) cannot exceed the triangular carrier slope
- The crossover frequency of the loop gain of Fig. 6 (bandwidth) cannot exceed half of the carrier triangular frequency.

With these constraints and the motor parameters given in Appendix A, the parameters for the PI controller are chosen as:

$$K_p = 862 \quad \text{and} \quad K_i = 288960$$

B. Proposed Flux Controller

The proposed flux controller is shown in Fig. 7 which in principle works similar to the torque controller. The flux error status and its average value are given by equation (11) and (12), respectively.

$$q_f(t) = \begin{cases} 1 & for \quad F_c \geq C_{upper} \\ 0 & for \quad F_c < C_{lower} \end{cases} \tag{11}$$

$$d_f(t) = \frac{1}{T_{tri}} \int_{t}^{t+T_{tri}} q(t)\, dt \tag{12}$$

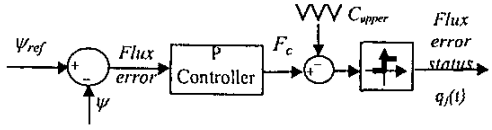

Fig 7. Proposed flux controller

The flux slopes are functions of sinus of the angle and repeats for every sector [7]. The average value of the flux slopes over a sector are given by (13) and (14) with the assumption that the slope is constant when the flux error status is 1 or 0.

$$\frac{d\psi^{+}}{dt} = \frac{1}{N_f}\sum_{n=0}^{N_f}\frac{2}{3}V_{dc}\sin\left(\frac{\pi}{3}\right)n = A_\psi \tag{13}$$

$$\frac{d\psi^{-}}{dt} = -\frac{1}{N_f}\sum_{n=0}^{N_f}\frac{2}{3}V_{dc}\sin\left[\left(\frac{\pi}{3}\right)n + \frac{2}{3}\pi\right] = B_\psi \tag{14}$$

The number of positive and negative slopes within a sector is denoted by $N_f = (2\pi f_{inv})/6\omega$. Equations (13) and (14) are then averaged as followed:

$$\frac{d\psi}{dt} = (A_\psi - B_\psi)t + B_\psi \tag{15}$$

The linearized flux loop is outlined in Fig. 8.

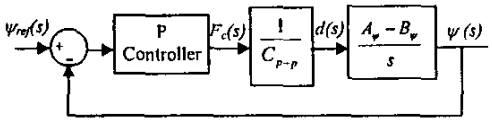

Fig. 8 Linearized flux loop

Since the openloop gain consists of only an integral and a gain, the flux loop only requires a propotional controller. The propotional gain, K_p is selected based on the following restriction:

- The absolute slop of stator flux, i.e. (13) and (14) must not exceed the triangular slope.
- The bandwidth is large enough to remove the ripple at $6f_e$ (synchronous frequency).

Based on the motor parameters, K_p is selected as 6900.

V. SIMULATION RESULTS

Simulation using Matlab/Simulink was carried out to verify the validity of the proposed methods. Three sets of simulation were performed to prove the feasibility of the proposed controller:

(i) hysteresis-based controllers,

(ii) proposed torque controller with hysteresis-based flux controller,

(iii) proposed torque and flux controllers.

The parameters of the motor and the proposed controllers are calculated as listed in Appendix A and B. The widths of the flux and torque hysteresis comparators are set to 5% of their rated values respectively.

Fig. 9 shows the torque response for the three set simulations mentioned above. By applying a ±0.5 Nm square-wave torque reference, it can be seen that a significant torque ripple reduction had been achieved. The results also indicated that the dynamic torque response of the proposed controller is as good as the hysteresis-based controller. Fig 9 (b) and (c) gain an almost same torque ripple however the proposed flux controller had also managed to reduce the flux ripple as well.

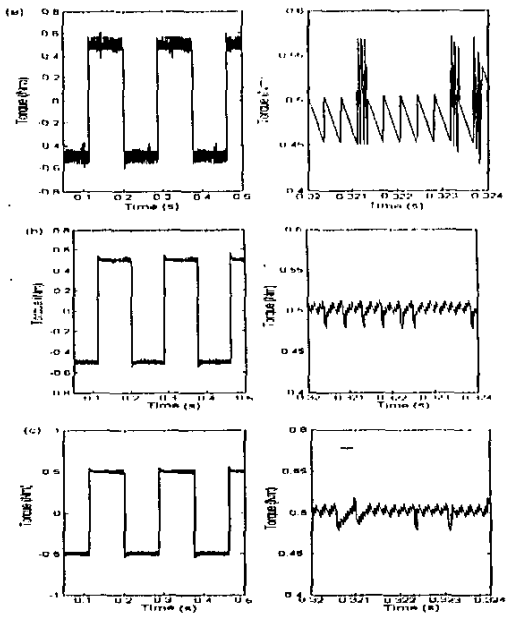

Fig. 9 Torque response and its zoom in view for (a) hysteresis-based controller, (b) proposed torque controller with hysteresis-based flux controller, (c) proposed torque and flux controllers

Fig. 10 (a) and (b) illustrate the torque error status for hysteresis-based controller and the upper triangular waveform with the compensated torque error signal, Tc for the proposed controller. Although the hysteresis torque band amplitude is set to 5%, but owing to the delay in feedback signal, a reverse voltage vector is selected. As a result, the torque ripple increases, as discussed in Section III. Fig 10(c) and (d) clearly indicate the significant reduction in torque ripple achieved using the proposed controllers.

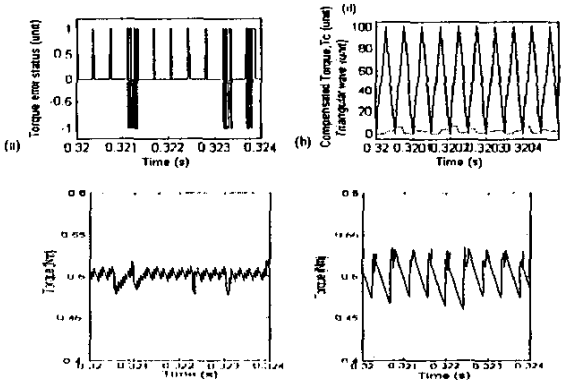

Fig. 10 (a) Torque error status for hysteresis-based controller, (b) Upper triangular waveform and T_c for proposed controller, Zoomed in torque for (c) proposed controllers, (d) hysteresis-based controller

Fig. 11 gives the simulation results of the speed response for the three sets of conditions to a square wave torque reference. The figure indicates the comparable dynamic speed response of the proposed controllers compared to the hysteresis-based controller.

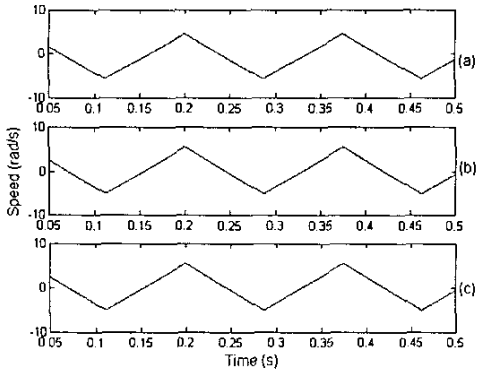

Fig. 11 Speed response for (a) hysteresis-based controller, (b) proposed torque controller with hysteresis-based flux controller, (c) proposed torque and flux controllers

The proposed flux controller gives not much affect to the torque ripple, however its contribution is more on stator flux ripple reduction. Fig 12 depicts the steady state flux locus for hysteresis-based controller, proposed torque controller with hysteresis-based flux controller and the proposed torque and flux controllers. Hysteresis-based controller introduces high ripples (Fig. 12(a)) while Fig. 12(b) gives a hexagonal shape, which will cause the actual torque contained harmonics at $6f_e$. It can be seen that the proposed controller obtains an almost circular locus in Fig.12(c).

The experimental set-up for the proposed controllers is currently under development. The proposed hardware implementation is a combination of hybrid analog and digital circuits utilizing Altera Field Programmable Gate Array (FPGA).

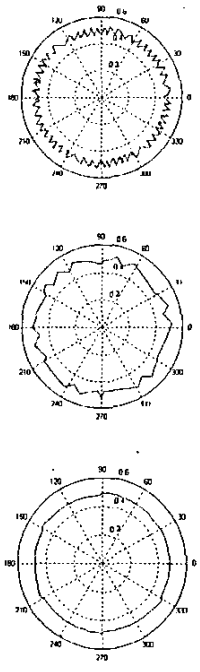

Fig. 12 Steady state flux locus for (a) hysteresis-based controller, (b) proposed torque controller with hysteresis-based flux controller, (c) proposed torque and flux controllers

VI. CONCLUSION

A new pair of torque and flux controllers, which minimizes the torque ripple, has been presented in this paper. Simulation results demonstrated that the proposed controllers produce an excellent performance in minimizing the torque and stator flux ripples and maintaining a constant switching frequency. Due to their simple structure, they can be easily implemented using analog/digital circuit, which is currently under development.

VII. APPENDIX

A. Motor parameter used for Simulation

DC link voltage, V_{dc}:	392V
Pole pair:	2
Stator resistance, R_s:	10.9Ω
Rotor resistance, R_r:	9.5Ω
Stator self-inductance, L_s:	859mH
Rotor self-inductance, L_r:	859mH
Mutual inductance, L_m:	828mH
Rated flux, ψ_{ref}:	0.495Wb

B. Parameters for the proposed controllers

(i)	Torque loop	
	A:	335
	B:	12
	K:	6
	Triangular frequency:	20kHz
(ii)	Flux loop	
	A:	226
	B:	226
	Triangular frequency:	10kHz

VIII. REFERENCES

[1] I. Takahashi , T. Noguchi, "A new quick-response and high-efficiency control strategy of an induction motor", *IEEE Trans. Ind. Appl.*, vol IA-22, No 5 Sept/Oct 1986

[2] P. Tiitinen, "The next generation motor control method, DTC direct torque control", *Proc. of Int. Conf on Power Electronics, Drives and Energy System for Industrial Growth*, N. Delhi, India, pp. 37-43, 1996.

[3] J-W. Kang and S. K. Sul, "Analysis and prediction of inverter switching frequency in direct torque control of induction machine based on hysteresis bands and machine parameters", IEEE Transactions on Industrial Electronics, Vol. 48, No. 3 , pp. 545 –553, Jun 2001

[4] J-W. Kang, D-W Chung and S. K. Sul, "Direct torque control of induction machine with variable amplitude control of flux and torque hysteresis bands", International Conference on Electric Machines and Drives IEMD '99 , pp. 640 –642, 1999.

[5] T. G. Habetler,. F. Profumo, M. Pastorelli and L. M. Tolbert, "Direct torque control of induction machines using space vector modulation", *IEEE Trans. Ind. Appl.*, Vol. 28, No. 5, pp. 1045-1053, 1992.

[6] Y. Li, J. Shao,. and B. Si, "Direct torque control of induction motors for low speed drives considering discrete effect of control and dead-time timing of inverters", *in Conf. Rec. IEEE-IAS Annual Meeting*, pp. 781-788, 1997.

[7] J. K. Kang. and S. K. Sul, "Torque ripple minimisation strategy for direct torque control of induction motor", *in Conf. Rec. IEEE-IAS Annual Meeting*, pp. 438-443, 1998

[8] S. Mir. and M. E. Elbuluk, "Precision torque control in inverter-fed induction machines using fuzzy logic", *In Conf. Rec. IEEE-IAS Annual Meeting*, pp. 396-401, 1995.

[9] I. G. Bird. and H. Zelaya De La Parra, "Fuzzy logic torque ripple reduction for DTC based AC drives", *Electronic Letters*, Vol. 33, No.17, pp. 1501-1502, 1997.

[10] D. Casadei,G. Serra and A. Tani, "Improvement of direct torque control performance by using a discrete SVM technique", 29th Annual IEEE Power Electronics Specialists Conference PESC 98, Vol. 2 , pp. 997-1003, 1998.

[11] N.R.N. Idris and A.H.M. Yatim, "Reduced Torque Ripple And Constant Torque Switching Frequency Strategy For Direct Torque Control Of Induction Machine", *In Conf Rec. IEEE-APEC*, pp. 154-161, vol .1, 2000.

[12] D. Casadei;G. Serra.and A. Tani "Analytical investigation of torque and flux ripple in DTC schemes for induction motors", 23rd International Conference on Industrial Electronics, Control and Instrumentation, IECON 97., Vol. 2 , pp. 552 -556, 1997

[13] A. Purcell and P. Acarnley, " Device switching scheme for direct torque control", Electronics Letters , Vol. 34, Issue 4 , pp. 412 -414, 1998.

[14] C. Lascu, I. Boldea, F. Blaabjerg, "A modified direct torque control (DTC) for induction motor sensorless drive", IEEE Industry Applications Conference Annual Meeting, Vol: 1 , pp. 415-422, 1998

[15] Yen-Shin Lai; Jian-Ho Chen; "A new approach to direct torque control of induction motor drives for constant inverter switching frequency and torque ripple reduction", IEEE Transactions on Energy Conversion, Vol. 16, No. 3, pp. 220-227, Sep 2001